nature structural & molecular biology

Helix movement is coupled to displacement of the second extracellular loop in rhodopsin activation

Shivani Ahuja[1], Viktor Hornak[2], Elsa C Y Yan[3,6], Natalie Syrett[4], Joseph A Goncalves[2], Amiram Hirshfeld[5], Martine Ziliox[2], Thomas P Sakmar[3], Mordechai Sheves[5], Philip J Reeves[4], Steven O Smith[2] & Markus Eilers[2]

The second extracellular loop (EL2) of rhodopsin forms a cap over the binding site of its photoreactive 11-*cis* retinylidene chromophore. A crucial question has been whether EL2 forms a reversible gate that opens upon activation or acts as a rigid barrier. Distance measurements using solid-state ^{13}C NMR spectroscopy between the retinal chromophore and the β4 strand of EL2 show that the loop is displaced from the retinal binding site upon activation, and there is a rearrangement in the hydrogen-bonding networks connecting EL2 with the extracellular ends of transmembrane helices H4, H5 and H6. NMR measurements further reveal that structural changes in EL2 are coupled to the motion of helix H5 and breaking of the ionic lock that regulates activation. These results provide a comprehensive view of how retinal isomerization triggers helix motion and activation in this prototypical G protein–coupled receptor.

G protein–coupled receptors (GPCRs) comprise the largest and most diverse superfamily of membrane receptors, with a simple architectural core of seven transmembrane helices (H1 to H7) connected by typically short extracellular and cytoplasmic loops. Sequence variability within the transmembrane helices and extracellular loops allow GPCRs to respond to diverse stimuli, including light and a wide variety of ligands. Small-molecule ligands can bind within the helical core of the receptor, whereas larger peptide and protein ligands bind at the extracellular loops. The second extracellular loop (EL2) in particular has been the target of a number of functional studies indicating that it has an integral role in activation of GPCRs that bind either small molecules or large peptide ligands[1–4].

The vertebrate visual pigments are unique in the class A GPCRs in that they are activated by photoreaction of an 11-*cis* retinylidene chromophore. The retinal is covalently attached via a protonated Schiff base (PSB) within the seven-transmembrane-helix bundle. The crystal structure of rhodopsin indicates that EL2 extends from Trp175 on H4 to Thr198 on H5. The intriguing aspect about the EL2 sequence is that it folds into a highly ordered and stable structure consisting of two short β-strands (β3 and β4) that form a lid over the retinal binding site[5,6]. EL2 is constrained by a conserved disulfide bond between Cys110 at the end of H3 and Cys187 on β4 that is crucial for the correct folding of rhodopsin[7,8]. Other than the Cys110-Cys187 disulfide bond, the EL2 sequence is not conserved among the class A GPCRs.

The structure of EL2 in rhodopsin is stabilized by several polar residues that form a well-defined hydrogen-bonded network (**Supplementary Fig. 1a** online). At the center of this network is Glu181 on the β3 strand. Glu181 is hydrogen-bonded to Tyr192 (β4) and Tyr268 (H6) and is connected through water-mediated hydrogen bonds to Ser186 (EL2) and to Glu113 (H3), the counterion to the retinal PSB[6]. Glu113 is hydrogen-bonded to the backbone carbonyl of Cys187 (EL2) through a water molecule and is within hydrogen-bonding distance to the hydroxyl group of Thr94 (H2)[6]. The involvement of Glu113 in this stable hydrogen-bonded network is important in raising the pK_a of the Schiff base (above 16)[9] and ensuring that it remains protonated in the dark state of rhodopsin[10,11]. Besides the conserved disulfide bond and the hydrogen-bonding network involving Glu181, there are a striking number of hydrogen-bonding interactions between the β-strands and the ends of the transmembrane helices (for example, Trp175-Ser202, Ser176-Thr198, Arg177-Asp190 and Tyr178-Ala168). Computational studies identified this region as part of a stable folding core of rhodopsin[12], suggesting that EL2 is important for maintaining a stable, inactive receptor conformation.

In contrast to the role of EL2 as a stable cap, several studies have suggested that EL2 is dynamic and mediates both receptor activity and ligand binding. It has been proposed that in the C5a receptor, EL2 serves as a negative regulator[3], by a mechanism where the loop inserts between the transmembrane helices to block receptor activity and then is released upon ligand binding. Other work suggested that a short EL2 in the melanocortin receptor, which is unable to insert into the helical transmembrane core, leads to a high level of constitutive activation[13]. In the recent crystal structure of the β2-adrenergic receptor (β2-AR)[14], EL2 is not closely associated with the ligand

[1]Departments of Physics and Astronomy, [2]Biochemistry and Cell Biology, Stony Brook University, Stony Brook, New York 11794-5215, USA. [3]Laboratory of Molecular Biology and Biochemistry, The Rockefeller University, 1230 York Avenue, New York, New York 10065, USA. [4]Department of Biological Sciences, University of Essex, Wivenhoe Park, Essex C04 3SQ, UK. [5]Department of Organic Chemistry, The Weizmann Institute, Rehovot 76100, Israel. [6]Present address: Department of Chemistry, Yale University, New Haven, Connecticut 06520, USA. Correspondence should be addressed to S.O.S. (steven.o.smith@sunysb.edu).

Received 31 August 2008; accepted 2 January 2009; published online 1 February 2009; doi:10.1038/nsmb.1549

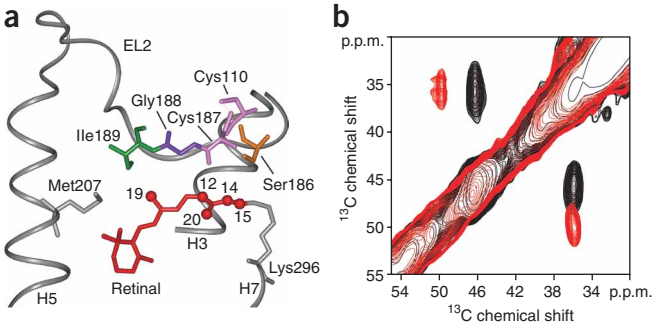

Figure 1 Structural changes involving the conserved Cys110-Cys187 disulfide link on activation of rhodopsin. (**a**) View of the β4 strand of EL2 from the rhodopsin crystal structure[6] highlighting the interactions of Ile189, Gly188, Cys187 and Ser186 with the polyene chain of the retinal. Cys110 on the extracellular end of H3 forms a conserved disulfide link with Cys187 in β4. (**b**) A region from the two-dimensional DARR NMR spectrum of rhodopsin, selectively labeled with ^{13}Cβ-cysteine. The figure highlights the cross-peak between Cys187 (46.8 p.p.m.) and Cys110 (36.4 p.p.m.) in rhodopsin (black). On conversion to meta II (red), there is a distinct shift in the cross-peak to 50.1 p.p.m. for Cys187. The ^{13}Cβ chemical shift of Cys110 at ~36 p.p.m. does not change appreciably between rhodopsin and meta II. The eight reduced cysteines in rhodopsin are observed as a broad resonance at ~25 p.p.m. (not shown).

binding site. The β2-AR structure, along with the observation that short loops may be correlated with constitutively active GPCRs, raises the question of whether the role of EL2 as a stable cap is unique in rhodopsin because of the crucial requirement that visual pigments must have very low basal activity in the dark.

Here we use ^{13}C magic angle spinning (MAS) NMR spectroscopy to address the position of EL2 in rhodopsin and in the active meta-rhodopsin II (meta II) intermediate, and show how motion of EL2 is coupled to motion of transmembrane helix H5 and the insertion of Tyr223 into the region of the 'ionic lock' between H3 and H6. We obtained retinal-protein and protein-protein distance constraints from NMR measurements for rhodopsin and meta II (**Supplementary Fig. 1b** and **Supplementary Table 1** online), and we used them to perform restrained molecular dynamic simulations to obtain an atomistic model of meta II. Chemical shift measurements of the conserved Cys110-Cys187 disulfide bond and distance measurements between the retinal chromophore and the β4 strand of EL2 are consistent with motion of EL2 away from the agonist all-*trans* retinal Schiff base upon receptor activation. Mutational studies on Glu181 (EL2) and Met288 (H7) show that the hydrogen-bonding network on EL2 is coupled to the hydrogen-bonding network centered on H5 involving His211, which in turn leads to rearrangement of the intracellular end of H5 in meta II. Together, these results explain how EL2 is a pivotal element in locking the extracellular ends of H5, H6 and H7 in inactive conformations in the dark and how EL2 motion allows the intracellular ends of these helices to shift into active conformations in the light.

RESULTS

Activation of rhodopsin is initiated by photoisomerization of its retinal chromophore within a tightly packed protein environment. Because the all-*trans* retinal chromophore in the active meta II intermediate does not fit in the retinal binding site of the dark-state of rhodopsin[15], conformational changes of a highly strained retinal must induce changes in the structure of the receptor to release the absorbed light energy.

EL2 is displaced from the retinal binding site in meta II

The first indication that the structure or position of EL2 changes in meta II arises from the large chemical shift changes observed for ^{13}Cβ-Ser186, ^{13}Cβ-Cys187 and ^{13}Cα-Gly188 (**Fig. 1a**). The Cys110-Cys187 disulfide bond is the only conserved feature in EL2. **Figure 1b** presents ^{13}C dipolar assisted rotational resonance (DARR) NMR spectra of rhodopsin (black) and meta II (red) labeled with ^{13}Cβ-cysteine. The β-carbon resonances in disulfide bonds occur in a unique chemical shift window (34–50 p.p.m.) and are sensitive to the secondary structure with a range of 34–43 p.p.m. for α-helices and 36–50 p.p.m. for β-sheets[16]. **Figure 1b** shows strong cross-peaks between the Cys110-Cys187 β-carbon resonances at 36.4 p.p.m. and 46.8 p.p.m., respectively. The 46.8-p.p.m. chemical shift of Cys187 is consistent with its location in the β4 strand of EL2. Upon conversion to meta II, the Cys187 resonance shifts to 50.1 p.p.m. owing to a change in the conformation of EL2 or a change in the environment around Cys187. The chemical shift of Cys110 does not change appreciably (−0.2 p.p.m.), indicating that the secondary structure of H3 near Cys110 does not change in meta II.

In addition to the chemical shift changes observed in Cys187, we observed an ~1.6-p.p.m. change in the ^{13}Cβ chemical shift of Ser186 and a 2.9-p.p.m. change in the ^{13}Cα resonance of Gly188 (**Supplementary Figs. 2** and **3** online). The ^{13}Cβ-Ser186 chemical shift change may be attributed to a change in the hydrogen-bonding interaction of Ser186 with surrounding residues on EL2 and H3, whereas the ^{13}Cα-Gly188 chemical shift is likely to be due to changes in backbone torsion angles.

Confirmation of the motion of EL2 away from the retinal binding site in meta II comes from direct distance measurements. The β4 strand of EL2 is aligned almost parallel to the retinal in the binding site, with Cys185 close to the PSB end of the retinal and with Ile189 close to the retinal β-ionone ring. We observed close contact between the retinal ^{13}C14 and ^{13}C15 carbons and ^{13}Cβ-Ser186 (**Fig. 2a**), between the retinal ^{13}C12 and ^{13}C20 carbons and ^{13}C1-Cys187 (**Fig. 2b**), and between the retinal ^{13}C12 and ^{13}C20 carbons and ^{13}Cα-Gly188 in rhodopsin (**Fig. 2c**). These contacts are lost in meta II. Moreover, we were not able to observe contacts in rhodopsin or meta II between the retinal ^{13}C9 and ^{13}C12 carbons and U-$^{13}C_6$-Ile189 (**Fig. 2d**).

As indicated above, in general we found that the distances obtained from NMR measurements on rhodopsin were comparable with the corresponding distances in the rhodopsin crystal structure before converting to meta II. The meta II intermediate that we trapped at low temperature in n-dodecyl-β-D-maltoside (DDM) was present in a single, well-defined state (Methods). We typically observed strong cross-peaks for ^{13}C-^{13}C distances of ~4.0 Å or less, moderate cross-peaks for distances of up to 5.0 Å and weak cross-peaks for distances of up to 6.0 Å. Consequently, the lack of contacts in meta II indicate that retinal-EL2 distances are on the order of 6.0 Å or more. In rhodopsin, we observed strong contacts between the ^{13}C1-Cys187 on EL2 and the retinal ^{13}C12 and ^{13}C20 carbons (**Fig. 2b**). In the rhodopsin crystal structure[6], Cys187 is 4.21 Å and 6.22 Å from the retinal C12 and C20 carbons, respectively. On conversion to meta II, we lost both retinal contacts with Cys187, consistent with an increase in separation between EL2 and the retinal.

Further support for separation between the retinal and EL2 in meta II comes from (i) the loss of tyrosine-glycine contacts in meta II and (ii) assignment of a cross-peak at 46.5 p.p.m. between the ^{13}C20 methyl carbon on the retinal and a ^{13}Cα-glycine residue. There are two

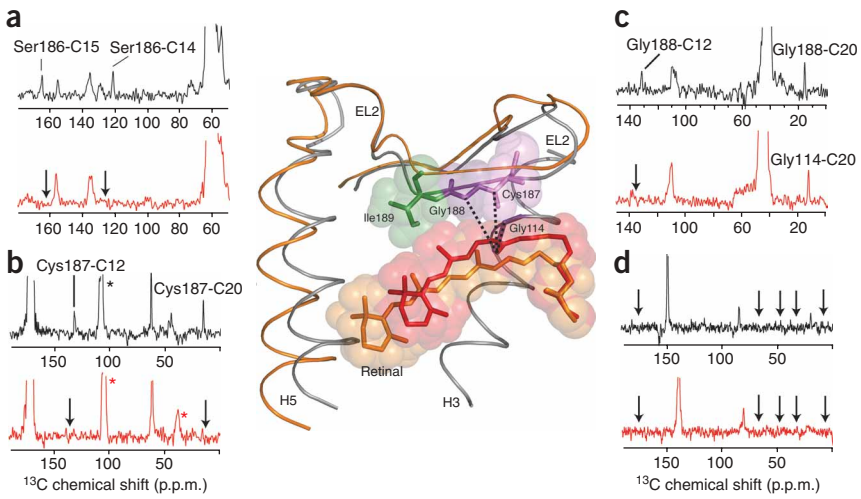

Figure 2 Two-dimensional ^{13}C DARR NMR spectra of retinal-EL2 interactions. Rows from the two-dimensional ^{13}C DARR NMR spectra of rhodopsin (black) and meta II (red) are shown. (**a**) Rhodopsin labeled with ^{13}Cβ-serine and ^{13}C14,15-retinal. Cross-peaks are observed between Ser186 (63.3 p.p.m.) and the ^{13}C14 and ^{13}C15 resonances in dark rhodopsin, which are lost (arrows) in meta II. (**b**) Rhodopsin labeled with ^{13}C1-cysteine and ^{13}C12,20-retinal. Cross-peaks are observed between Cys187 (170.8 p.p.m.) and the ^{13}C12 and ^{13}C20 resonances in dark rhodopsin, which are lost (arrows) in meta II. Asterisks correspond to MAS side bands. (**c**) Rhodopsin labeled with ^{13}Cα-glycine and ^{13}C12,20-retinal. Cross-peaks are observed between Gly188 (42.0 p.p.m.) and the ^{13}C12 and ^{13}C20 resonances in dark rhodopsin, which are lost (arrows) in meta II. However, a new Gly-C20 contact is observed in meta II, which is assigned to Gly114 (see text). (**d**) Rhodopsin labeled with U-$^{13}C_6$-isoleucine and ^{13}C9-retinal. No contacts were observed between Ile189 and C9 on the polyene chain of the retinal in either rhodopsin (black arrows) or meta II (red arrows). The structure of EL2 in rhodopsin is shown (center), indicating the contacts observed between the C20 methyl group and Cys187, Gly188 and Gly114 in rhodopsin. To illustrate the displacement of EL2 that is needed to satisfy the NMR constraints, we have superimposed the rhodopsin crystal structure (gray) with the meta II model (orange) obtained from molecular dynamic simulations guided by our experimentally determined retinal-protein contacts.

tyrosine-glycine contacts that connect EL2 with the extracellular ends of transmembrane helices H3 and H6, namely Tyr268-Gly188 and Tyr178-Gly114. Both contacts are lost in meta II (**Supplementary Fig. 3**). There are only two glycines in the binding cavity close to the C20 methyl group: Gly114 on H3 and Gly188 on EL2 (**Fig. 3**). In meta II, we assign the C20-glycine cross-peak to Gly114 (H3) based on the presence of this resonance in the two-dimensional DARR spectrum of the G188A mutant of meta II. The assignment of a C20-Gly114 contact in meta II indicates that the C20-Gly188 contact is lost despite the large rotation of the C20 methyl group toward EL2 (**Supplementary Figs. 4** and **5** online).

The model in **Figure 2** shows the crystal structure of rhodopsin containing the 11-*cis* (red) retinal PSB tightly packed against EL2. The distances between the C20 methyl group and the ^{13}C-labeled positions on Gly114, Cys187 and Gly188 are shown. Cross-peaks between the retinal C20 methyl group and each of these amino acids were observed in the dark. We superimposed the position of the all-*trans* retinal SB (orange) in meta II predicted using restrained molecular dynamic simulations (**Supplementary Table 1**). To satisfy distance constraints derived from our NMR measurements, in the molecular dynamic simulations the retinal shifted slightly toward the cytoplasmic side of the binding site and EL2 moved toward the extracellular surface.

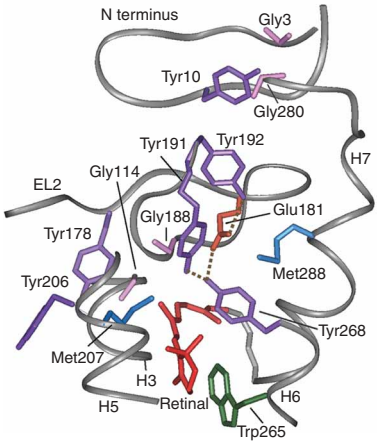

Figure 3 A view of the extracellular side of rhodopsin from the crystal structure[6]. The figure highlights the relative position of six tyrosine residues: Tyr10, Tyr178, Tyr191, Tyr192, Tyr206 and Tyr268. Of these tyrosines, Tyr191, Tyr192 and Tyr268 are involved in the hydrogen-bonding network with Glu181. Tyr268 and Tyr191 are also in close contact with Met288 on H7. Tyr206 on H5 is involved in a second hydrogen-bonding network with His211 (H5), Glu122 (H3), Trp126 (H3) and Ala166 (H4) (not shown). Additionally, the figure shows tyrosine-glycine interactions on the extracellular side of rhodopsin between Gly188-Tyr268, Gly3-Tyr10-Gly280 and Gly114-Tyr178.

Rearrangement of hydrogen-bonding networks involving EL2-H5

The loss of EL2-retinal contacts in meta II and the changes observed in the chemical shifts for the β4 strand indicate that EL2 changes position upon receptor activation. As a result, the next question to be investigated concerned whether the hydrogen-bonding network involving EL2 remains intact or is disrupted in meta II.

Tyrosine residues are an integral part of the EL2 hydrogen-bonding network[6] (**Fig. 3**). The ^{13}Cζ resonances of the 18 tyrosines in rhodopsin are not resolved (**Fig. 4a**, black). However, the difference spectrum between rhodopsin and meta II highlights the ^{13}Cζ-tyrosine resonances that change upon rhodopsin activation (**Fig. 4b**). There are two well-resolved shoulders in the meta II portion of the difference spectrum (**Fig. 4b**). The distinct meta II resonance at 153.6 p.p.m. is readily assigned to Tyr206 on H5 on the basis of the loss of a Cζ-tyrosine resonance at 153.6 p.p.m. in the meta II component of the Y206F mutant difference spectrum (**Fig. 4c**). Additional support for this assignment is provided in **Supplementary Figure 6** online. The upfield shift of ^{13}Cζ-Tyr206 resonance is consistent with a weaker Cζ-OH hydrogen bond in meta II.

The downfield resonance at 159.3 p.p.m. is reflective of a more strongly hydrogen-bonded tyrosine[17]. Both tyrosines with unusual chemical shifts must be coupled to the hydrogen-bonding network involving Glu181 on EL2, because both resonances were lost in the

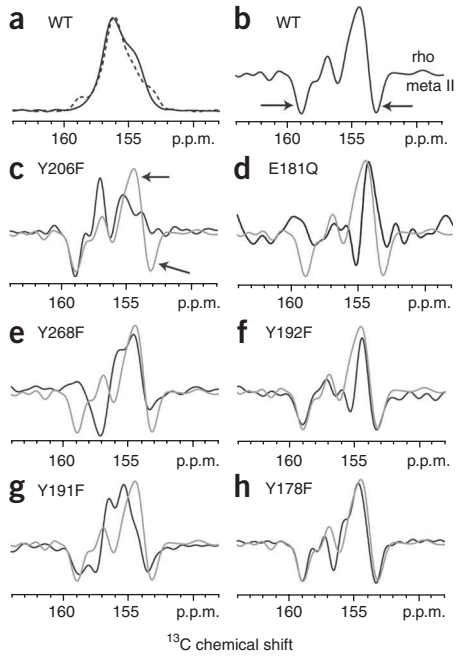

Figure 4 One dimensional ^{13}C cross-polarization magic angle spinning (CP-MAS) spectra of rhodopsin and meta II labeled with ^{13}Cζ-tyrosine. (**a**) Overlap of the ^{13}C one-dimensional CP-MAS spectra of the ^{13}Cζ-tyrosine resonance in rhodopsin (rho, solid line) and meta II (broken line). (**b**–**h**) Difference spectra for wild-type (WT) rhodopsin (**b**) and several rhodopsin mutants, Y206F (**c**), E181Q (**d**), Y268F (**e**), Y192F (**f**), Y191F (**g**) and Y178F (**h**). The wild-type difference spectrum is shown in gray in **c**–**h**.

tyrosine difference spectrum of the E181Q mutant (**Fig. 4d**). There is no evidence for a tyrosinate anion[18], which would have shown a chemical shift closer to 165 p.p.m.[17].

To assign the tyrosine resonance at 159.3 p.p.m. in meta II, we collected difference spectra for a series of rhodopsin mutants (Y268F, Y192F, Y191F and Y178F) in which tyrosine residues in the retinal binding cavity near Glu181 were mutated individually to phenylalanine (**Fig. 4e–h**). None of the ^{13}Cζ-tyrosine difference spectra shows a complete loss of the negative peak at 159.3 p.p.m., except for the Y268F mutant spectrum, in which the negative peak at 159.3 p.p.m. seems to shift to 157.5 p.p.m. We are not able to assign the 159.3-p.p.m. resonance to Tyr268 because of the appearance of a positive peak at 159.3 p.p.m. in the dark spectrum of the Y268F mutant, which suggests that mutation of Tyr268 causes another tyrosine in the vicinity to become more strongly hydrogen-bonded. In the difference spectrum of the Y191F mutant, the negative peak at ~159 p.p.m. is split into two components as compared to the wild-type difference spectrum.

The loss of the 159.3-p.p.m. resonance in the E181Q mutant and its sensitivity to mutation of Tyr268 and Tyr191 strongly suggest an assignment to one of the tyrosines associated with EL2. This assignment is supported by two-dimensional DARR data obtained on rhodopsin labeled with ^{13}Cζ-tyrosine and ^{13}Cε-methionine. In the rhodopsin crystal structure (PDB 1U19), there are five Met(^{13}Cε)-Tyr(^{13}Cζ) pairs (Met288-Tyr268, 3.9 Å; Met207-Tyr191, 4.8 Å; Met288-Tyr191, 5.2 Å; Met253-Tyr306, 5.5 Å; Met288-Tyr192, 5.7 Å). In **Figure 5a**, we observe two cross-peaks between tyrosine and methionine that we assign to the closest methionine-tyrosine pairs (that is, Met288-Tyr268 and Met207-Tyr191). Conversion to meta II generated a cross-peak between the tyrosine resonance at 159.3 p.p.m. and a methionine resonance at 12.8 p.p.m. We can assign this methionine to Met288 on H7 based on the loss of this cross-peak in the M288L mutant (**Fig. 5b**, orange).

The M288L data along with the tyrosine difference spectra above indicate that the 159.3-p.p.m. resonance belongs to either Tyr191 or Tyr268 in meta II. We assume that the strong hydrogen-bonding interaction for a tyrosine at 159.3 p.p.m. is due to its interaction with Glu181 and that the appearance of a resonance at 159.3 p.p.m. in the Y268F rhodopsin spectrum and in the Y191F meta II spectrum occurs because these mutations lead to the rearrangement of the EL2 hydrogen-bonding network. We assign the 159.3-p.p.m. resonance in meta II to Tyr191, because we observe a cross-peak at 156.5 p.p.m. between a tyrosine and the retinal C20 methyl group[19] that we assign

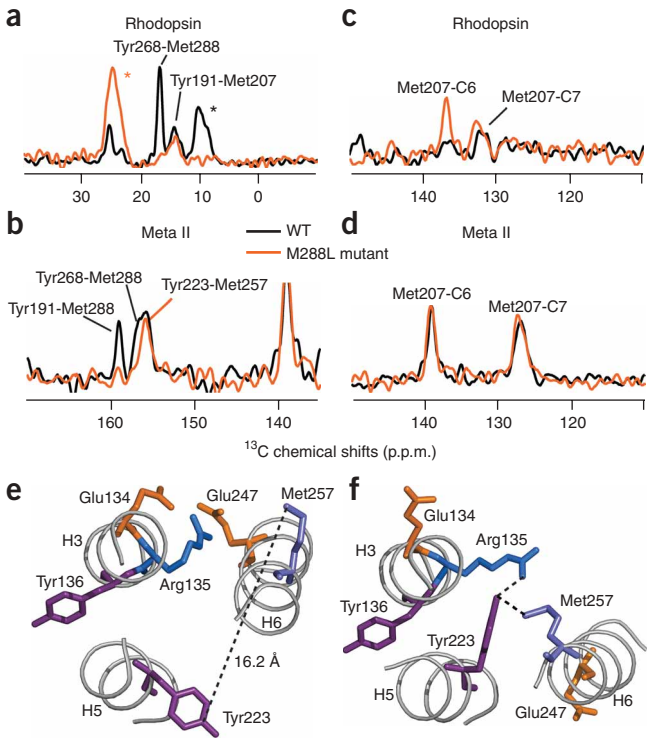

Figure 5 Two-dimensional DARR NMR of Tyr(Cζ)-Met(Cε) contacts in rhodopsin and the M288L rhodopsin mutant. (**a**) Rows through the ^{13}Cζ-tyrosine diagonal resonance from two-dimensional DARR NMR spectra of rhodopsin (black) and the M288L rhodopsin mutant (orange) labeled with ^{13}Cζ-tyrosine and ^{13}Cε-methionine. Asterisks correspond to MAS side bands. (**b**) Rows through the ^{13}Cε-Met diagonal resonance from two-dimensional DARR NMR spectra of wild-type meta II (WT, black) and the M288L rhodopsin mutant (orange) following conversion to meta II. (**c**) Rows through the ^{13}Cε-methionine diagonal resonance of rhodopsin (black) and the M288L rhodopsin mutant (orange) showing the cross-peaks to the retinal ^{13}C6 and ^{13}C7 resonances. (**d**) Same as in **c** following conversion to meta II. In the M288L mutant of rhodopsin, we observe a contact between Met207 and C6 that is not present in wild-type rhodopsin. This change in the Met207-retinal contact in the M288L mutant of rhodopsin can be interpreted as either a change in the position of the retinal or in the position of Met207 on H5 upon mutation of Met288 (H7) to leucine. Upon activation, the Met207-retinal interactions in the M288L mutant are identical to those in wild-type meta II. (**e**) A view of the ionic lock between Arg135 and Glu247 from the crystal structure of rhodopsin[20]. The Tyr223-Met257 distance is well beyond the range of the DARR NMR experiment. (**f**) Structure of the ionic lock from the recent crystal structure of opsin[21,22] showing the close proximity between Tyr223 and Met257.

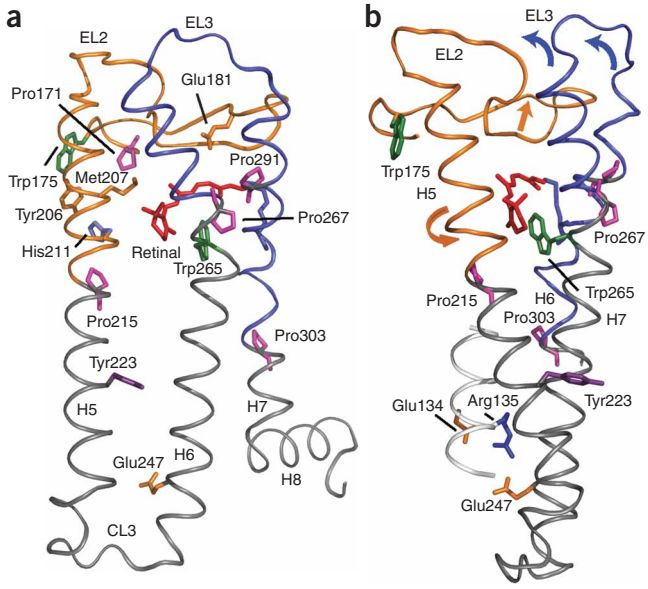

Figure 6 Crystal structure of rhodopsin[20] highlighting EL2 and H5. (**a**) Retinal isomerization within the tightly packed binding site results in steric contacts between the β-ionone ring and H5 and between the retinal C19 and C20 methyl groups and EL2. These interactions trigger the simultaneous displacement of EL2 and H5. Motion of the β-ionone ring is also coupled to the motion of Trp265. Trp265 is packed against the β-ionone ring and C20 of the retinal, as well as Gly121 on H3 and Ala295 on H7. Movement of the Trp265 side chain away from these crucial contacts allows helices H6 and H7 to shift into active conformations. The coupled motions of helices H5-H7, in turn, are coupled to the rearrangement of electrostatic interactions involving the conserved ERY sequence at the cytoplasmic end of H3, exposing the G protein binding site on the cytoplasmic surface of the protein. (**b**) View of the rhodopsin crystal structure highlighting the interaction between EL2 and EL3 on the extracellular side of the receptor, and the positions of Tyr223 and the conserved Glu135-Arg135-Tyr136 sequence on the intracellular side of the receptor.

to Tyr268. The C20 methyl group is closer to Tyr268 (4.2 Å) than to Tyr191 (8.0 Å) in rhodopsin, and we expect that motion of EL2 away from the retinal would only increase the ^{13}C20-Tyr191(^{13}Cζ) distance. Together, these data argue that Tyr191 becomes more strongly hydrogen-bonded in meta II and that the hydrogen-bonding network involving the tyrosines and Glu181 on EL2 remains intact.

Coupling of EL2 displacement to rotation of helix H5

The data presented above on the E181Q and M288L mutants and in **Supplementary Figure 3** on the Y206F mutant suggest that light-induced structural changes in EL2 are strongly coupled to the hydrogen-bonding network centered on H5. First, in the E181Q mutant (**Fig. 4d**) the resonance at 153.6 p.p.m. assigned to Tyr206 (H5) is lost. Second, in the M288L (H7) mutant a contact is gained between the ε-CH_3 group of Met207 (H5) and the retinal C6 carbon (**Fig. 5c**). Third, in the Y206F (H5) mutant a tyrosine-glycine contact is lost that is likely to involve Tyr10 or Tyr29 on the extracellular loops of rhodopsin, as there are no glycines in the vicinity of Tyr206.

We propose that the functional unit is the EL2-H5 sequence. The crystal structure of rhodopsin shows that the β-strands in EL2 are extensively knit together by hydrogen-bonding interactions that extend to Tyr268 on H6 and Glu113 on H3 (refs. 6,20). If the motion of EL2 is coupled to the motion of H5, then the Pro170-Pro171 sequence at the H4-β3 boundary may serve as a hinge, leading to observable changes in the hydrogen-bonding interactions that link β3 to H4 and H4 to H5. We observe that many of the hydrogen-bonding contacts involving the extracellular ends of H4 and H5 change in meta II (**Supplementary Fig. 1a**).

We have previously shown that H5 undergoes a change in orientation in the region of His211 (**Supplementary Fig. 6**). **Figure 5e,f** shows how rotation of H5 leads to disruption of the ionic lock between H3 and H6. In the dark state of rhodopsin (**Fig. 5e**), Arg135 of the conserved ERY sequence on H3 interacts with Glu247 (H6). In the recent structure of opsin (**Fig. 5f**) with[21] and without[22] the Gα peptide bound, H5 is rotated and Tyr223 (a residue that is highly conserved across the GPCR family) interacts directly with Arg135 and Met257 on H6. The Tyr223-Arg135 interaction is thought to be one element in breaking the ionic lock and stabilizing the active conformation of rhodopsin. **Figure 5b** shows a new tyrosine-methionine contact in meta II that we can assign to the Tyr223-Met257 interaction, consistent with the proposal that this active-state geometry is maintained in the opsin structure[22]. Notably, mutation of Tyr223 to phenylalanine results in an appreciable increase in the decay rate of meta II to opsin (**Supplementary Fig. 7** online), in agreement with the idea that the Tyr223-Arg135 interaction stabilizes the active conformation of the receptor. These results indicate that there are two crucial H3-H5 interactions that hold helix H5 in an active geometry: Glu122-His211 (refs. 23,24) and Arg135-Tyr223 (refs. 21,22). The model of activation that emerges from these studies is one where steric contacts between the retinal β-ionone ring with H5 and the retinal C19 methyl group with EL2 shift the EL2-H5 sequence into an active geometry stabilized by H3-H5 contacts; retinals lacking either the ring[25] or the C19 methyl group[26] fail to activate rhodopsin, and mutation of Tyr223 to phenylalanine leads to rapid meta II decay.

DISCUSSION

EL2 controls access to the retinal binding site

The main conclusion from our studies is that EL2 changes position upon activation and that this change is coupled to motion of transmembrane helix H5. We have recently defined the location of the retinal chromophore in meta II (S.A., E. Crocker, M.E., P.J.R., M.S. and S.O.S., unpublished data), and our current measurements between the β4 strand and the retinal indicate that there must be an increase in the separation between the retinal and EL2 upon activation. The hydrogen-bonding network involving Glu181 seems to remain intact in meta II, and consequently the displacement of EL2 does not seem to be large.

Our observations can be compared with the crystal structures of opsin[22] and a 'photoactivated' (deprotonated) intermediate of rhodopsin[27]. In these structures, EL2 does not seem to have moved to any appreciable extent. The differences between meta II and opsin suggest that the all-*trans* retinal Schiff base holds EL2 in an active conformation in meta II. Release of the retinal to form opsin allows the binding-site residues to rearrange and EL2 to shift back to roughly its position in rhodopsin.

The displacement of EL2 away from the retinal that we observed is consistent with studies showing that the retinal binding site becomes more accessible to water and hydroxylamine in meta II[28,29]. Mutation of many of the residues in the hydrogen-bonding network involving EL2, such as Glu181 (ref. 30) and Tyr192 (ref. 31), results in increased accessibility of the retinal PSB to hydroxylamine in the dark. Also, the appearance of an N-D amide A vibration at 2,366 cm^{-1} in meta II has been attributed to hydrogen-deuterium exchange that occurs

following the exposure of the EL2 β-hairpin to water in the meta I–to–meta II transition[32]. Notably, neither disruption of the Cys110-Cys187 disulfide bond by mutation to alanine nor disruption of the salt bridge between Arg177 and Asp190 on EL2 increases hydroxylamine accessibility[33,34], suggesting that the hydrogen-bonding network involving Glu181 is alone sufficient to keep EL2 tightly capped over the retinal binding site.

In a parallel fashion, EL2 may serve to control the access of small-molecule ligands to interior binding sites within the ligand-activated GPCRs. For example, alanine-scanning mutagenesis of the M1 muscarinic acetylcholine receptor revealed that the access of ligands to the binding site was increased by mutation of EL2 residues[35]. Furthermore, substituted-cysteine accessibility studies of the dopamine D2 receptor showed that the extracellular part of H5 is accessible to hydrophilic reagents[36]. Finally, the recent crystal structure of β2AR with a bound partial inverse agonist[14] shows that EL2 does not cap the amine binding site, as occurs in rhodopsin. Taken together, the studies on GPCRs activated by small-molecule ligands suggest that there is a dynamic role of EL2 in allowing water and ligands to enter the interior binding sites.

EL2 as a negative regulator in GPCR activation

Several studies have suggested that EL2 serves a role as a negative regulator in the class A GPCRs. The simple idea is that EL2 has multiple interactions with the extracellular ends of the transmembrane helices in the inactive state and that displacement of EL2 upon ligand binding allows H5, H6 and H7 to adopt active conformations. For example, one report showed that a high degree of constitutive activity is associated with the mutation of residues in EL2 of the C5a receptor[3]. The authors proposed that mutation of EL2 increases the flexibility of the loop and releases inhibitory constraints. The high degree of basal activity in the melanocortin receptor, which has a short EL2 and lacks the conserved disulfide bond, was explained by a related mechanism[13]. Finally, cross-linking in the putative ligand binding site[37,38] and metal binding sites[39] in the vicinity of EL2 modulate receptor activity. These modifications were designed to mimic the movement of the transmembrane helices, and for this to occur, EL2 was envisioned to change conformation or position.

In rhodopsin, EL2 has also been implicated as a negative regulator of receptor activity. Mutation of Tyr191 and Tyr192 to leucine decreases the stability of the binding pocket, leading to faster meta II decay rates[40], and mutation of Ser186 to alanine and Glu181 to phenylalanine strongly perturbs the kinetics of rhodopsin activation[41]. However, none of the EL2 mutants tested in rhodopsin shows constitutive activity. This may be due to the presence of additional regulatory elements, such as the interaction between the retinal PSB and its Glu113 counterion and the tight packing between the 11-*cis* retinal and conserved Trp265 (H6), which all contribute to low dark noise in rhodopsin.

EL2-H5 as a structural unit in GPCRs

One of the challenges in understanding the mechanism of GPCR activation is to establish how retinal isomerization[42,43] or ligand binding[39,44] produces rigid-body motion of the transmembrane helices. Our results suggest that the motion of EL2 is coupled to the motion of H5 and breaking of the ionic lock.

Tight coupling between EL2 and H5 is supported in studies on ligand-activated GPCRs[45–48]. One study addressed the coupling of EL2 and H5 by replacing the EL2-H5 sequence from the $5HT_{1D}$ serotonin receptor with the corresponding sequence from the $5HT_{1B}$ serotonin receptor[46]. The authors found that it was necessary to replace the entire EL2-H5 sequence to recover antagonist binding; replacing either the EL2 or H5 sequence alone markedly decreased binding. Also, the idea that EL2 is a structured unit is reflected in gonadotrophin-releasing hormone receptor studies showing that exchange of the entire EL2 from another species had less effect on ligand binding affinity than point mutations of EL2 within a species[48].

Figure 6 highlights the helix-loop-helix (HLH) segments involving EL2 and EL3. Motion of EL2 away from the retinal binding site is coupled to the outward displacement of the extracellular end of H5 and the inward displacement and rotation of the intracellular end of H5 (refs. 21,22). The outward displacement of H5 is driven by steric interaction with the retinal β-ionone ring and is stabilized by a direct Glu122-His211 interaction. Motion of EL2 may allow the extracellular end of the H6-EL3-H7 segment to pivot toward the center of the protein and conversely allow the intracellular end of H6 to rotate outward[42,49]. Inward motions of the extracellular ends of H6 and H7 are captured in the global toggle switch model of GPCR activation[39].

Additionally, **Figure 6** shows the positions of key tryptophan residues in rhodopsin, Trp265 (H6) and Trp175 (H4). Trp265 is conserved throughout the class A GPCRs and is an important element of the activation mechanism of rhodopsin[50]. Trp175 is located at the junction of EL2 with H4 and H5. In rhodopsin, the W175F mutation is one of the only mutations in the H4-EL2-H5 segment that leads to constitutive activity[51]. The fact that this tryptophan residue is highly conserved in the visual receptors, but not in other class A GPCRs, suggests that the H4-EL2-H5 sequence up to Pro215 is specific to different subfamilies of class A GPCRs.

In conclusion, the structural constraints described above provide insights into how EL2 and its extensive hydrogen-bonding interactions are involved in coupling retinal isomerization to the activation of rhodopsin. The subfamily-specific H4-EL2-H5 unit in rhodopsin holds H5 and the extracellular ends of H6 and H7 in inactive conformations. Retinal isomerization and displacement of EL2 from the retinal binding site are coupled to motion of H5 and to the inward motion of the H6-EL3-H7 unit. Similar motions are likely to occur in other GPCRs[39,52], suggesting that EL2 may act as a plug or cork that must be released or rearranged for receptor activation.

METHODS

Expression and purification of ^{13}C-labeled rhodopsin. We used a stable tetracycline-inducible HEK293S cell line[53] containing the bovine opsin gene or its mutants[54] to express rhodopsin. The cells were grown in DMEM[55] prepared from cell culture–tested components (Sigma). Suspension cultures were grown using a bioreactor in medium with specific ^{13}C-labeled amino acids (Cambridge Isotope Laboratories), heat-inactivated FBS (10% (v/v), dialyzed three times against 20 liters PBS per liter of serum)[56], 0.1% (w/v) Pluronic F-68, 300 mg l^{-1} dextran sulfate, 100 units ml^{-1} penicillin and 100 μg ml^{-1} streptomycin. On day 4 after incubation, cells were fed with 2.4 g l^{-1} glucose. Opsin gene expression was induced 5 d after inoculation by addition of both 2 mg l^{-1} tetracycline and 5 mM sodium butyrate (final concentration) to the growth medium[53], and cells were harvested on day 7.

We resuspended the HEK293S cell pellets in 40 ml PBS per liter of cell culture plus protease inhibitors[54] and added unlabeled 11-*cis* retinal in two steps to a final concentration of 15 μM. The rhodopsin-containing cells were solubilized in 40 ml of PBS plus 1% (w/v) DDM per liter of cell culture for 4 h at room temperature (22–25 °C). We carried out subsequent purification by immunoaffinity chromatography using the rho-1D4 antibody (National Cell Culture Center) as described previously[54]. The eluted rhodopsin fractions were pooled and concentrated to a final volume of ~400 μl using 10-kDa MWCO Centricon devices (Amicon).

Synthesis of ^{13}C-labeled retinals and regeneration into rhodopsin. We synthesized specific ^{13}C-labeled retinals by previously described methods[57,58] and purified them using HPLC as previously described[50].

We carried out regeneration of the rhodopsin pigments with ^{13}C-labeled retinal in DDM micelles by illuminating the concentrated samples containing a 2:1 molar ratio of labeled retinal to protein, as described previously[19]. Typically, more than 85% of the sample was regenerated with labeled retinal. Different regeneration rates were observed for wild-type and mutant opsins. A stream of argon gas was used to evaporate the regenerated sample down to a volume of 60 µl.

Solid-state NMR spectroscopy. Concentrated samples (7–10 mg) were loaded into 4-mm MAS zirconia rotors. All NMR spectra were acquired at a static magnetic field strength of 14.1 T (600 MHz) on a Bruker AVANCE spectrometer using double-channel 4 mm MAS probes, as described previously[50]. Typically, we used MAS spinning rates of 8–12 kHz. One-dimensional ^{13}C spectra were acquired using ramped amplitude cross-polarization, with contact times of 2 ms and acquisition times on the order of 16 ms for all experiments. Intermolecular ^{13}C-^{13}C distance constraints on rhodopsin in the inactive and the active state were obtained using the DARR recoupling technique with a mixing time of 600 ms to maximize homonuclear recoupling between different ^{13}C labels. The ^{1}H radiofrequency field strength during mixing was matched to the MAS speed for each sample, satisfying the $n = 1$ matching condition. Two-pulse phase-modulated or SPINAL64 proton decoupling was typically used during the evolution and acquisition periods, with a radiofrequency field strength of 80–90 kHz. In each two-dimensional data set, we acquired 1,024 time domain points in the f2 (direct) dimension and 64 points in the f1 (indirect) dimension. All experiments were conducted at −80 °C. ^{13}C spectra were referenced externally to the carbonyl resonance of powdered glycine at 176.46 p.p.m. relative to neat TMS at 0.0 p.p.m.

Trapping of the metarhodopsin II intermediate. Samples were illuminated for 45–60 s at room temperature in the NMR rotor using a 400-W lamp with a >495-nm cutoff filter and immediately placed in the NMR probe with the probe stator warmed to 5 °C. Under slow spinning (~2 kHz), the sample was frozen within 3 min of illumination using nitrogen gas cooled to −80 °C. To confirm that meta II conversion was complete and stably trapped, we monitored the chemical shift changes of the ^{13}C-labeled carbons of the polyene chain of the retinal, as they are sensitive to both protonation and isomerization. The linewidths of the resolved protein and retinal NMR resonances were generally between 1 p.p.m. and 2 p.p.m. in both rhodopsin and meta II. The absence of line broadening or resonance splitting indicates that a spectroscopically well-defined meta II state has been trapped. The time between illumination and freezing of the sample was approximately 3 min, indicating that the proton uptake in our sample was complete; the intermediate we trapped is functionally equivalent to meta II in rod outer segment (ROS) membranes, as it can activate transducin[59]. Also, it has been shown that the vibrational frequencies observed in the Fourier transform infrared (FTIR) difference spectrum of meta II minus rhodopsin are identical for rhodopsin in DDM or ROS membranes[60].

Note: Supplementary information is available on the Nature Structural & Molecular Biology website.

ACKNOWLEDGMENTS

This work was supported by the US National Insitutes of Health (NIH)–National Science Foundation instrumentation grants (S10 RR13889 and DBI-9977553), a grant from the NIH to S.O.S. (GM-41412), and a grant from the US-Israel Binational Science Foundation to M.S. We thank C.A. Opefi for help with the M288A and M288L mutants and gratefully acknowledge the W.M. Keck Foundation for support of the NMR facilities in the Center of Structural Biology at Stony Brook. M.S. acknowledges support from the Kimmelman Center for Biomolecular Structure and Assembly.

Published online at http://www.nature.com/nsmb/
Reprints and permissions information is available online at http://npg.nature.com/reprintsandpermissions/

1. Samson, M. *et al.* The second extracellular loop of CCR5 is the major determinant of ligand specificity. *J. Biol. Chem.* **272**, 24934–24941 (1997).
2. Shi, L. & Javitch, J.A. The second extracellular loop of the dopamine D-2 receptor lines the binding-site crevice. *Proc. Natl. Acad. Sci. USA* **101**, 440–445 (2004).
3. Klco, J.M., Wiegand, C.B., Narzinski, K. & Baranski, T.J. Essential role for the second extracellular loop in C5a receptor activation. *Nat. Struct. Mol. Biol.* **12**, 320–326 (2005).
4. Scarselli, M., Li, B., Kim, S.K. & Wess, J. Multiple residues in the second extracellular loop are critical for M-3 muscarinic acetylcholine receptor activation. *J. Biol. Chem.* **282**, 7385–7396 (2007).
5. Palczewski, K. *et al.* Crystal structure of rhodopsin: a G protein-coupled receptor. *Science* **289**, 739–745 (2000).
6. Okada, T. *et al.* The retinal conformation and its environment in rhodopsin in light of a new 2.2 Å crystal structure. *J. Mol. Biol.* **342**, 571–583 (2004).
7. Karnik, S.S. & Khorana, H.G. Assembly of functional rhodopsin requires a disulfide bond between cysteine residues 110 and 187. *J. Biol. Chem.* **265**, 17520–17524 (1990).
8. Hwa, J., Klein-Seetharaman, J. & Khorana, H.G. Structure and function in rhodopsin: mass spectrometric identification of the abnormal intradiscal disulfide bond in misfolded retinitis pigmentosa mutants. *Proc. Natl. Acad. Sci. USA* **98**, 4872–4876 (2001).
9. Steinberg, G., Ottolenghi, M. & Sheves, M. pKa of the protonated Schiff base of bovine rhodopsin: a study with artificial pigments. *Biophys. J.* **64**, 1499–1502 (1993).
10. Sakmar, T.P., Franke, R.R. & Khorana, H.G. The role of the retinylidene Schiff base counterion in rhodopsin in determining wavelength absorbance and Schiff base pKa. *Proc. Natl. Acad. Sci. USA* **88**, 3079–3083 (1991).
11. Cohen, G.B., Oprian, D.D. & Robinson, P.R. Mechanism of activation and inactivation of opsin: role of Glu113 and Lys296. *Biochemistry* **31**, 12592–12601 (1992).
12. Rader, A.J. *et al.* Identification of core amino acids stabilizing rhodopsin. *Proc. Natl. Acad. Sci. USA* **101**, 7246–7251 (2004).
13. Holst, B. & Schwartz, T.W. Molecular mechanism of agonism and inverse agonism in the melanocortin receptors—Zn^{2+} as a structural and functional probe. *Ann. NY Acad. Sci.* **994**, 1–11 (2003).
14. Cherezov, V. *et al.* High-resolution crystal structure of an engineered human β_2-adrenergic G protein-coupled receptor. *Science* **318**, 1258–1265 (2007).
15. Matsumoto, H. & Yoshizawa, T. Recognition of opsin to longitudinal length of retinal isomers in formation of rhodopsin. *Vision Res.* **18**, 607–609 (1978).
16. Sharma, D. & Rajarathnam, K. ^{13}C NMR chemical shifts can predict disulfide bond formation. *J. Biomol. NMR* **18**, 165–171 (2000).
17. Herzfeld, J. *et al.* Solid-state ^{13}C NMR study of tyrosine protonation in dark-adapted bacteriorhodopsin. *Biochemistry* **29**, 5567–5574 (1990).
18. DeLange, F. *et al.* Tyrosine structural changes detected during the photoactivation of rhodopsin. *J. Biol. Chem.* **273**, 23735–23739 (1998).
19. Patel, A.B. *et al.* Coupling of retinal isomerization to the activation of rhodopsin. *Proc. Natl. Acad. Sci. USA* **101**, 10048–10053 (2004).
20. Li, J., Edwards, P.C., Burghammer, M., Villa, C. & Schertler, G.F.X. Structure of bovine rhodopsin in a trigonal crystal form. *J. Mol. Biol.* **343**, 1409–1438 (2004).
21. Scheerer, P. *et al.* Crystal structure of opsin in its G-protein-interacting conformation. *Nature* **455**, 497–502 (2008).
22. Park, J.H., Scheerer, P., Hofmann, K.P., Choe, H.W. & Ernst, O.P. Crystal structure of the ligand-free G-protein-coupled receptor opsin. *Nature* **454**, 183–187 (2008).
23. Patel, A.B. *et al.* Changes in interhelical hydrogen bonding upon rhodopsin activation. *J. Mol. Biol.* **347**, 803–812 (2005).
24. Imai, H. *et al.* Single amino acid residue as a functional determinant of rod and cone visual pigments. *Proc. Natl. Acad. Sci. USA* **94**, 2322–2326 (1997).
25. Jäger, F. *et al.* Interactions of the β-ionone ring with the protein in the visual pigment rhodopsin control the activation mechanism. An FTIR and fluorescence study on artificial vertebrate rhodopsins. *Biochemistry* **33**, 7389–7397 (1994).
26. Ganter, U.M., Schmid, E.D., Perez-Sala, D., Rando, R.R. & Siebert, F. Removal of the 9-methyl group of retinal inhibits signal transduction in the visual process. A Fourier transform infrared and biochemical investigation. *Biochemistry* **28**, 5954–5962 (1989).
27. Salom, D. *et al.* Crystal structure of a photoactivated deprotonated intermediate of rhodopsin. *Proc. Natl. Acad. Sci. USA* **103**, 16123–16128 (2006).
28. Sakmar, T.P., Franke, R.R. & Khorana, H.G. Glutamic acid-113 serves as the retinylidene Schiff base counterion in bovine rhodopsin. *Proc. Natl. Acad. Sci. USA* **86**, 8309–8313 (1989).
29. Zhukovsky, E.A. & Oprian, D.D. Effect of carboxylic acid side chains on the absorption maximum of visual pigments. *Science* **246**, 928–930 (1989).
30. Yan, E.C.Y. *et al.* Function of extracellular loop 2 in rhodopsin: glutamic acid 181 modulates stability and absorption wavelength of metarhodopsin II. *Biochemistry* **41**, 3620–3627 (2002).
31. Janz, J.M. & Farrens, D.L. Role of the retinal hydrogen bond network in rhodopsin Schiff base stability and hydrolysis. *J. Biol. Chem.* **279**, 55886–55894 (2004).
32. Furutani, Y., Shichida, Y. & Kandori, H. Structural changes of water molecules during the photoactivation processes in bovine rhodopsin. *Biochemistry* **42**, 9619–9625 (2003).
33. Davidson, F.F., Loewen, P.C. & Khorana, H.G. Structure and function in rhodopsin: replacement by alanine of cysteine residues 110 and 187, components of a conserved disulfide bond in rhodopsin, affects the light-activated metarhodopsin II state. *Proc. Natl. Acad. Sci. USA* **91**, 4029–4033 (1994).
34. Janz, J.M., Fay, J.F. & Farrens, D.L. Stability of dark state rhodopsin is mediated by a conserved ion pair in intradiscal loop E-2. *J. Biol. Chem.* **278**, 16982–16991 (2003).
35. Goodwin, J.A., Hulme, E.C., Langmead, C.J. & Tehan, B.G. Roof and floor of the muscarinic binding pocket: variations in the binding modes of orthosteric ligands. *Mol. Pharmacol.* **72**, 1484–1496 (2007).

36. Javitch, J.A., Fu, D. & Chen, J. Residues in the fifth membrane-spanning segment of the dopamine D2 receptor exposed in the binding-site crevice. *Biochemistry* **34**, 16433–16439 (1995).
37. Struthers, M., Yu, H.B. & Oprian, D.D. G protein-coupled receptor activation: analysis of a highly constrained, "straitjacketed" rhodopsin. *Biochemistry* **39**, 7938–7942 (2000).
38. Han, S.J. *et al.* Identification of an agonist-induced conformational change occurring adjacent to the ligand-binding pocket of the M-3 muscarinic acetylcholine receptor. *J. Biol. Chem.* **280**, 34849–34858 (2005).
39. Elling, C.E. *et al.* Metal ion site engineering indicates a global toggle switch model for seven-transmembrane receptor activation. *J. Biol. Chem.* **281**, 17337–17346 (2006).
40. Doi, T., Molday, R.S. & Khorana, H.G. Role of the intradiscal domain in rhodopsin assembly and function. *Proc. Natl. Acad. Sci. USA* **87**, 4991–4995 (1990).
41. Yan, E.C.Y. *et al.* Photointermediates of the rhodopsin S186A mutant as a probe of the hydrogen-bond network in the chromophore pocket and the mechanism of counterion switch. *J. Phys. Chem. C* **111**, 8843–8848 (2007).
42. Farrens, D.L., Altenbach, C., Yang, K., Hubbell, W.L. & Khorana, H.G. Requirement of rigid-body motion of transmembrane helices for light activation of rhodopsin. *Science* **274**, 768–770 (1996).
43. Sheikh, S.P., Zvyaga, T.A., Lichtarge, O., Sakmar, T.P. & Bourne, H.R. Rhodopsin activation blocked by metal-ion-binding sites linking transmembrane helices C and F. *Nature* **383**, 347–350 (1996).
44. Sheikh, S.P. *et al.* Similar structures and shared switch mechanisms of the β_2-adrenoceptor and the parathyroid hormone receptor—Zn(II) bridges between helices III and VI block activation. *J. Biol. Chem.* **274**, 17033–17041 (1999).
45. Olah, M.E., Jacobson, K.A. & Stiles, G.L. Role of the 2nd extracellular loop of adenosine receptors in agonist and antagonist binding—analysis of Chimeric A_1/A_3-adenosine receptors. *J. Biol. Chem.* **269**, 24692–24698 (1994).
46. Wurch, T., Colpaert, F.C. & Pauwels, P.J. Chimeric receptor analysis of the ketanserin binding site in the human 5-hydroxytryptamine$_{1D}$ receptor: importance of the second extracellular loop and fifth transmembrane domain in antagonist binding. *Mol. Pharmacol.* **54**, 1088–1096 (1998).
47. Conner, M. *et al.* Systematic analysis of the entire second extracellular loop of the V-1a vasopressin receptor—key residues, conserved throughout a G-protein-coupled receptor family, identified. *J. Biol. Chem.* **282**, 17405–17412 (2007).
48. Pfleger, K.D.G., Pawson, A.J. & Millar, R.P. Changes to gonadotropin-releasing hormone (GnRH) receptor extracellular loops differentially affect GnRH analog binding and activation: evidence for distinct ligand-stabilized receptor conformations. *Endocrinology* **149**, 3118–3129 (2008).
49. Altenbach, C., Kusnetzow, A.K., Ernst, O.P., Hofmann, K.P. & Hubbell, W.L. High-resolution distance mapping in rhodopsin reveals the pattern of helix movement due to activation. *Proc. Natl. Acad. Sci. USA* **105**, 7439–7444 (2008).
50. Crocker, E. *et al.* Location of Trp265 in metarhodopsin II: implications for the activation mechanism of the visual receptor rhodopsin. *J. Mol. Biol.* **357**, 163–172 (2006).
51. Madabushi, S. *et al.* Evolutionary trace of G protein-coupled receptors reveals clusters of residues that determine global and class-specific functions. *J. Biol. Chem.* **279**, 8126–8132 (2004).
52. Holst, B., Elling, C.E. & Schwartz, T.W. Partial agonism through a zinc-ion switch constructed between transmembrane domains III and VII in the tachykinin NK1 receptor. *Mol. Pharmacol.* **58**, 263–270 (2000).
53. Reeves, P.J., Kim, J.M. & Khorana, H.G. Structure and function in rhodopsin: a tetracycline-inducible system in stable mammalian cell lines for high-level expression of opsin mutants. *Proc. Natl. Acad. Sci. USA* **99**, 13413–13418 (2002).
54. Reeves, P.J., Thurmond, R.L. & Khorana, H.G. Structure and function in rhodopsin: high level expression of a synthetic bovine opsin gene and its mutants in stable mammalian cell lines. *Proc. Natl. Acad. Sci. USA* **93**, 11487–11492 (1996).
55. Dulbecco, R. & Freeman, G. Plaque production by the polyoma virus. *Virology* **8**, 396–397 (1959).
56. Eilers, M., Reeves, P.J., Ying, W.W., Khorana, H.G. & Smith, S.O. Magic angle spinning NMR of the protonated retinylidene schiff base nitrogen in rhodopsin: expression of ^{15}N-lysine and ^{13}C-glycine labeled opsin in a stable cell line. *Proc. Natl. Acad. Sci. USA* **96**, 487–492 (1999).
57. Lugtenburg, J. The synthesis of ^{13}C-labeled retinals. *Pure Appl. Chem.* **57**, 753–762 (1985).
58. Crocker, E. *et al.* Dipolar assisted rotational resonance NMR of tryptophan and tyrosine in rhodopsin. *J. Biomol. NMR* **29**, 11–20 (2004).
59. Han, M., Groesbeek, M., Smith, S.O. & Sakmar, T.P. Role of the C9 methyl group in rhodopsin activation: characterization of mutant opsins with the artificial chromophore 11-*cis*-9-demethylretinal. *Biochemistry* **37**, 538–545 (1998).
60. Fahmy, K. *et al.* Protonation states of membrane-embedded carboxylic acid groups in rhodopsin and metarhodopsin II: a Fourier-transform infrared spectroscopy study of site-directed mutants. *Proc. Natl. Acad. Sci. USA* **90**, 10206–10210 (1993).